Solid-Phase Organometallic Synthesis

Katja Heinze*[a]

Abstract: A solid-phase synthesis approach for a class of molybdenum carbonyl complexes has been developed. The system can be used to perform metal-complexation, ligand substitution reactions and oxidative eliminations on the solid phase and to cleave the final complexes under mild and selective conditions. Comparison is made to corresponding soluble complexes and liquid-phase reactions.

Keywords: immobilization · molybdenum · polymer-bound complexes · polymer-bound ligands · solid-phase synthesis

Introduction

Solid-phase organic synthesis (SPOS, Scheme 1) has become an increasingly useful method in synthetic organic and biological (especially pharmaceutical) chemistry. Generally, the compounds synthesised on the solid phase are *organic*

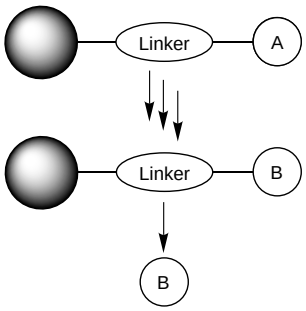

Scheme 1. Principle of solid-phase synthesis.

molecules, while "*organometallic* compounds are usually generated on insoluble supports as synthetic intermediates only, and not as target molecules".[1] A few exceptions are the solid-phase syntheses of metal complex functionalised oligonucleotides and oligodesoxynucleotides using standard DNA/RNA syntheses,[2] metal complex functionalised peptides using standard peptide chemistry,[3] and an attempt to prepare a 2,2′-bipyridine–dichloroplatinum derivative.[4]

Metal complexes have found applications as linkers[5] and as cleavage reagents[1, 6] in solid-phase chemistry, but the most important and most frequent use of metal complexes in this context is catalysis. In this case the metal complex remains bound to the solid support.

Coordination and organometallic chemistry on the solid phase has not yet been extensively explored, usually only the catalyst performance itself has been studied. Elementary reaction steps such as ligand substitution have not yet been investigated in detail under solid-phase reaction conditions despite the fact that in some cases catalytic results, activity and (enantio-) selectivity, are strikingly different when compared with the homogeneous case.[7]

In solid-phase chemistry the support can render increased stability to reactive intermediates by blocking bimolecular reaction steps[8] and can even change reaction pathways from ionic to radical mechanisms.[9] With this background in mind it appears useful and necessary to investigate elementary *inorganic* reaction steps performed on the insoluble support and to compare these results with conventional liquid-phase inorganic chemistry.

For this purpose a system has been designed, which makes it possible to perform standard reactions of coordination and organometallic chemistry under solid-phase reaction conditions and—for ease of reaction control and characterisation—to cleave the metal complexes from the solid phase.

The target molecules investigated herein are molybdenum carbonyl complexes, which have several important properties: 1) stability, 2) rich coordination chemistry, 3) CO ligands that serve as a sensitive analytical probe (IR), and 4) an NMR-active metal nucleus. In addition to these intrinsic properties molybdenum carbonyl complexes with nitrogen donor ligands have found applications as catalysts in allylic substitution reactions,[10] as cocatalysts for olefin metathesis,[7c] and they have proven useful for luminescence and electron transfer studies.[11]

Results and Discussion

Solution chemistry, ligand synthesis: The ligands employed are the bidentate nitrogen base **1a** with a phenolic hydroxy

[a] Dr. K. Heinze
Anorganisch-chemisches Institut der Universität Heidelberg
Im Neuenheimer Feld 270, 69120 Heidelberg (Germany)
Fax: (+49) 6221-545707
E-mail: katja@sun0.urz.uni-heidelberg.de

Supporting information for this article is available on the WWW under http://www.wiley-vch.de/home/chemistry/ or from the author.

  0947-6539/01/0713-2922 $ 17.50+.50/0

group for attachment on the solid support and the trimethylsilyl (TMS)-protected analogue **2a** as a model for the immobilised compounds (Scheme 2).

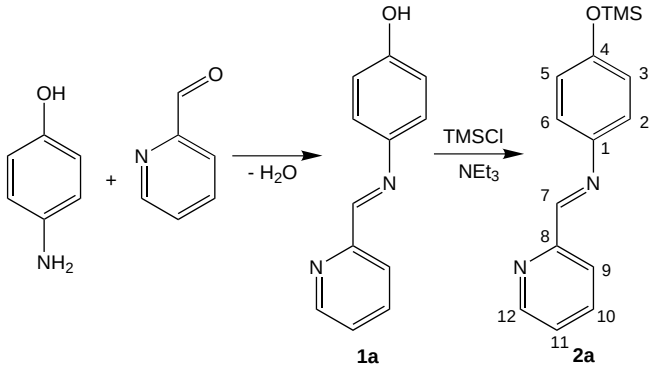

Scheme 2. Syntheses of ligands **1a** and **2a**.

Schiff base condensation of *p*-aminophenol and pyridine-2-carbaldehyde gives the chelating ligand **1a** and silylation of **1a** with trimethylsilyl chloride and triethylamine as the base resulted in the model analogue **2a** (Scheme 2). Both compounds are fully characterised (see Experimental Section).

Solution chemistry, model complexes: Common synthetic approaches to complexes of the type $(N\frown N')Mo(CO)_3L$ ($N\frown N'$ = symmetrical or asymmetrical bidentate nitrogen donor ligand, L = monodentate ligand) are depicted in Scheme 3.[12] All of them use high temperature or give only the tetracarbonyl compounds (L = CO), which then have to be converted into the desired tricarbonyl compounds—again using high temperature and rather harsh oxidative reaction conditions.

For a successful use in solid-phase chemistry with polystyrene resins, such harsh conditions have to be avoided as the molybdenum precursors can react with the aromatic residues of the support. Therefore a selective high-yield route using mild reaction conditions was elaborated with $[(CH_3CN)_3Mo(CO)_3]$ as the "$Mo(CO)_3$" source (Scheme 3, lower right).

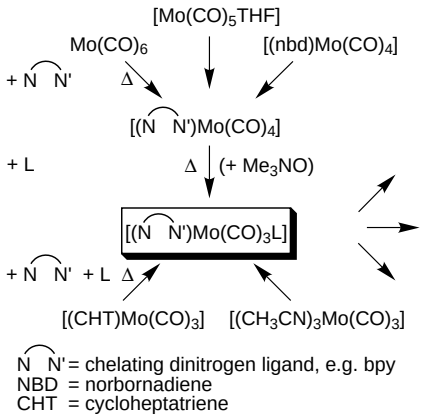

Scheme 3. Synthetic approaches to complexes of the type $[(N\frown N')Mo(CO)_3L]$.

Reaction of **1a**/**2a** with tris(acetonitrile)molybdenumtricarbonyl in acetonitrile at room temperature rapidly and cleanly gives the intensely blue-coloured complexes **1b**/**2b** in good to excellent yields (Scheme 4).

When the same reactions are performed in CH_2Cl_2 the tetracarbonyl complexes **1c**/**2c** are formed as shown by IR, UV/Vis/NIR, and NMR spectroscopy (Scheme 5). The latter reaction is always observed when dissolving complexes **1b**/**2b** in CH_2Cl_2. CO scrambling promoted by dichloromethane has been observed previously.[12a]

UV/Vis/NIR spectroscopy indicates the stoichiometric formation of **1c**/**2c** (final absorbance at 539 nm) plus an unidentified side product without carbonyl groups (as shown by IR spectroscopy; isosbestic point at 1821 cm^{-1}; see Supporting Information). The absence of well-defined isosbestic points (Figure 1, top) additionally indicates a complex reaction. From the absorbance changes at 500 and 539 nm a pseudo-first-order rate constant for the formation of **2c** can be obtained $k = 0.9 \times 10^{-4}\ s^{-1}$ (500 nm; $R^2 = 0.9993$) and $k = 1.1 \times 10^{-4}\ s^{-1}$ (539 nm; $R^2 = 0.9978$) in good agreement (Figure 1, bottom). For complex **1b** this reaction proceeds even faster, precluding a reliable rate constant determination but giving the same results with respect to the stoichiometry of the reaction.

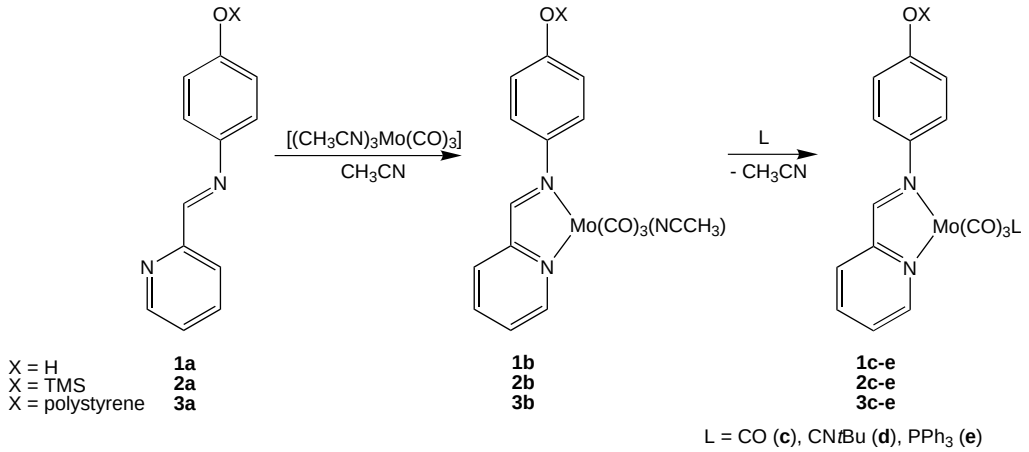

Scheme 4. Syntheses of soluble and immobilised complexes.

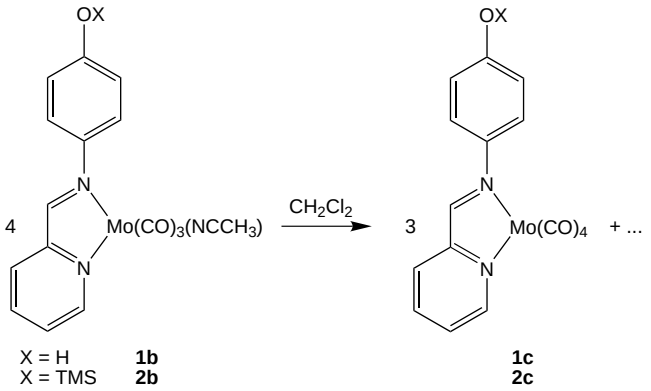

Scheme 5. Reaction of **1b**/**2b** to **1c**/**2c** in CH_2Cl_2.

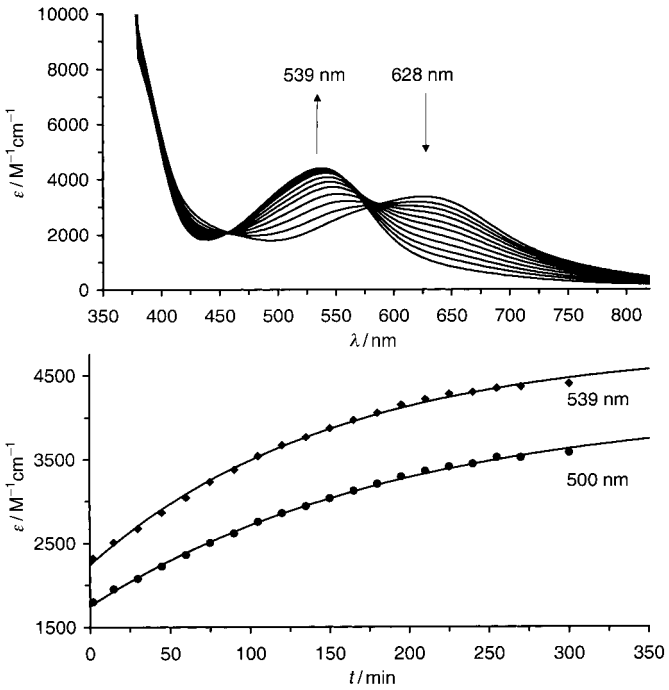

Figure 1. UV/Vis/NIR spectra of complex **2b** in CH_2Cl_2 (top) and the course for the formation of **2c** as a function of time (bottom).

The substitutional lability of the acetonitrile ligand in **1b** and **2b** has been utilised for ligand-exchange reactions with carbon monoxide, *tert*-butyl isonitrile, and triphenylphosphane giving the corresponding complexes **1c**–**e** and **2c**–**e**, respectively (Scheme 4). Reaction of **1c** with phenyltin trichloride as an example of an oxidative elimination gives the seven-coordinate molybdenum complex **1f**, while starting from **2c** does not produce the corresponding complex **2f** but rather **1f**, as the trimethylsilyl group is cleaved under these conditions (Scheme 6). All complexes have been thoroughly characterised by spectroscopic and analytical methods (Tables 1–3).

For **2e** the ^{13}C resonance signals of the CO groups are split into doublets by coupling to the ^{31}P nucleus. Coupling of the phosphorus atom is also observed to H^7 ($^4J_{P,H} = 2.6$ Hz; confirmed by a ^{31}P-^1H COSY experiment) and to C^7 ($^3J_{P,C} = 3.0$ Hz) of the Schiff base ligand. Complexes **1e**/**2e** each show

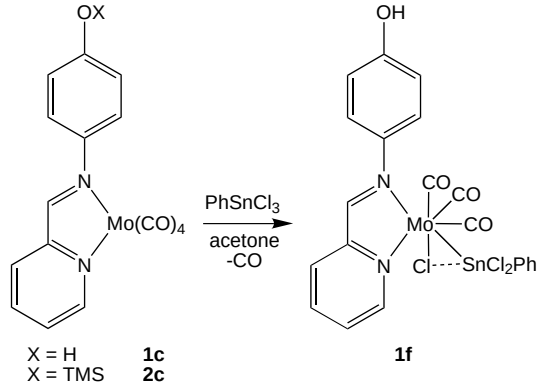

Scheme 6. Synthesis of **1f**.

a singlet in the ^{31}P NMR spectrum, confirming the presence of only one isomer.

The ^{95}Mo NMR signals (Table 2) appear in the expected region.[12f, 13] The different ligands L induce the expected high field shift of the ^{95}Mo resonances as well as of the ^{13}C

Table 1. ^1H NMR data for complexes **1b**–**1f** and **2b**–**2e** in CD_2Cl_2.[a]

	1b[b]	**1c**	**1d**	**1e**	**1f**[c]	**2b**[b]	**2c**	**2d**	**2e**
H^2/H^6	7.56 (d, 8.5 Hz)	7.55 (d, 8.7 Hz)	7.57 (d, 8.2 Hz)	7.37 (d, 8.2 Hz)	7.41 (d, 8.4 Hz)	7.59 (d, 8.8 Hz)	7.54 (d, 8.1 Hz)	7.58 (d, 8.5 Hz)	7.39 (d, 8.4 Hz)
H^3/H^5	6.91 (d, 8.5 Hz)	7.00 (d, 8.7 Hz)	6.99 (d, 8.2 Hz)	6.92 (d, 8.2 Hz)	6.87 (d, 8.4 Hz)	6.97 (d, 8.8 Hz)	7.01 (d, 8.1 Hz)	6.98 (d, 8.5 Hz)	6.94 (d, 8.4 Hz)
H^7[e]	8.65 (s)	8.57 (s)	8.56 (s)	8.18 (bs)	8.64 (s)	8.68 (s)	8.58 (s)	8.57 (s)	8.18 (d,[d])
H^9[e]	7.9–8.1 (m)	7.92 (d, 7.4 Hz)	7.89 (d, 8.0 Hz)	7.44 (d, 8.0 Hz)	8.09 (d, 7.2 Hz)	7.94 (d, 7.2 Hz)	7.9–8.0 (m)	7.9–8.0 (m)	7.45 (d, 8.0 Hz)
H^{10}		8.02 (pt)	7.91 (pt)	7.68 (pt)	8.21 (pt)	8.03 (pt)			7.68 (pt)
H^{11}	7.50 (pt)	7.56 (pt)	7.42 (pt)	7.01 (pt)	7.78 (pt)	7.50 (pt)	7.52 (pt)	7.42 (pt)	7.03 (pt)
H^{12}	9.03 (d, 5.0 Hz)	9.21 (d, 4.8 Hz)	9.23 (d, 4.6 Hz)	8.76 (d, 4.4 Hz)	9.10 (d, 4.8 Hz)	9.03 (d, 5.2 Hz)	9.20 (d, 3.8 Hz)	9.23 (d, 4.8 Hz)	8.77 (d, 4.8 Hz)
OH/OTMS	7.1 (bs)	n. o.	n. o.	n. o.	8.87 (s)	0.31 (s)	0.38 (s)	0.38 (s)	0.42 (s)
ligand L	1.92 (CH_3, s)	–	1.33 (CH_3, s, 9H)	7.19–7.23 (m, 15H)	7.38 ($C^o + C^p$, m, 3H) 8.00 (C^m, m, 2H)	1.93 (CH_3, s)	-	1.33 (CH_3, s, 9H)	7.1–7.3 (m, 15H)

[a] pt = pseudo-triplet; bs = broad singlet; n. o. = not observed. [b] In CD_3CN. [c] In [D_8]THF. [d] $^4J_{P,H} = 2.6$ Hz. [e] The cisoid conformation of the Schiff base ligand in the complexes is evidenced in solution by the observation of an NOE between H^7 and H^9 which is absent in the spectra of the free ligands.

0947-6539/01/0713-2924 $ 17.50+.50/0 *Chem. Eur. J.* **2001**, *7*, No. 13

Table 2. ^{13}C, ^{95}Mo, ^{31}P, and ^{119}Sn NMR data for complexes **1b**, **1f**, and **2b**–**2e** in CD_2Cl_2.[a]

	1b[b]	**1f**[c]	**2b**[b]	**2b**[d]	**2c**	**2d**	**2e**
C^1	145.5	149.8	146.8	145.9	146.4	146.9	146.6
C^2/C^6	124.7	124.4	124.6	123.6	123.8	123.8	124.4
C^3/C^5	116.4	116.7	121.0	120.4	120.8	120.5	120.5
C^4	155.8	154.1	155.8	155.1	154.8	155.0	154.3
C^7	162.6	166.6	163.2	160.6	160.9	159.2	158.6 (d, $^3J_{P,C}=3.0$ Hz)
C^8	158.3	157.9	156.6	156.2	156.6	156.2	156.3
C^9	129.2	130.4	129.3	128.1	128.6	128.1	128.0
C^{10}	138.7	141.7	138.7	137.3	137.4	136.4	135.3
C^{11}	127.6	130.0	127.8	126.6	126.8	125.9	125.7
C^{12}	152.7	154.3	152.8	152.3	153.4	152.5	152.3
OTMS	–	–	0.13	0.11	0.28	0.29	0.36
C^{13}/C^{15}	228.9/ 231.1	224.9[e] 227.7[e]	228.8/ 231.1	228.8/ 230.7	222.2/ 224.8	227.2/ 230.3	227.8 (d, $^2J_{P,C}=10.0$ Hz)/ 230.7 (d, $^2J_{P,C}=8.5$ Hz)
C^{14}	219.0	215.1 [e]	218.8	217.0	203.6	210.4	213.5 (d, $^2J_{P,C}=35.0$ Hz)
ligand L		143.8 (C^i)		1.95 (CH_3)		30.9 (CH_3)	134.1 (C^i, d, $^1J_{P,C}=28.0$ Hz)
		129.2 (C^o, $^2J_{Sn,C}=87$ Hz [f])		116.9 (C_q)		56.5 (C_q)	133.4 (C^o, d, $^2J_{P,C}=12.5$ Hz)
		136.2 (C^m, $^3J_{Sn,C}=61$ Hz [f])					128.4 (C^m, d, $^3J_{P,C}=8.5$ Hz)
		130.6 (C^p, $^4J_{SnC}=18$ Hz [f])					129.3 (C^p, s)
^{95}Mo δ ($\Delta\nu_{1/2}$/ Hz)	−969 (50)	n. o. [g]	−953 (65)	−933 (80)	−1160 (80)	−1095 (130)	−1043 (80) [h]
^{31}P δ ($\Delta\nu_{1/2}$/ Hz)	–	–	–	–	–	–	39.4 (4)
^{119}Sn δ ($\Delta\nu_{1/2}$/ Hz)	–	30 (265)	–	–	–	–	–

[a] Assignments are based on the intensity, chemical shifts, and DEPT and 2D NMR experiments. [b] In CD_3CN. [c] In [D_8]THF. [d] Due to the long acquisition time the ^{13}C and ^{95}Mo NMR spectra in CD_2Cl_2 additionally show signals of the tetracarbonyl complex **2c** but these are easily distinguished from those of **2b**. [e] At 193 K; not observed at 303 K. [f] ^{119}Sn satellites. [g] n. o. = not observed. [h] $^1J_{Mo,P}=138$ Hz.

Table 3. IR, UV/Vis/NIR and CV data ($E_{1/2}$ vs. SCE) for complexes **1b**–**1f** and **2b**–**1e** in CH_2Cl_2.

	$\tilde{\nu}_{CO}$ [cm^{-1}] (CH_2Cl_2/CsI)	$\tilde{\nu}_{CN}$ (CH_2Cl_2/CsI)	$\tilde{\nu}_{OH}$ (CH_2Cl_2/CsI)	λ_{max} [nm] (ε_{max} [$M^{-1}cm^{-1}$])	$E_{1/2}$ [mV] ($\Delta E_{1/2}$ [mV])
1b	1909 (vs), 1835 (sh), 1794 (vs)[a]/ 1898 (vs), 1833 (sh), 1782 (vs)	–	– 3230 (br)	589 (4400)[a] [624 in CH_2Cl_2]	+185 (110, qrev.)
1c	2016 (m), 1910 (vs), 1889 (sh), 1839 (s)/ 2018 (m), 1898 (vs), 1876 (vs), 1835 (vs), 1814 (vs)	–	– 3550 (m)	537 (4700)	+650 (100, qrev.)
1d	1917 (vs), 1833 (s), 1803 (s)/ 1935 (vs), 1919 (vs), 1867 (vs), 1763 (vs)[b]	2138 (s)/ 2122 (s)	– 3434 (s)	618 (6740)	+250 (85, qrev.)
1e	1919 (vs), 1827 (s), 1800 (s)/ 1911 (vs), 1823 (vs), 1765 (vs)	–	– 3448 (m)	615 (6145)	+365 (120, qrev.)
1f	2010 (vs), 1930 (m), 1907 (s)/ 2009 (vs), 1926 (m), 1905 (vs)	–	– 3444 (m)	474 (2515)	−850 mV (irrev.; +40 mV)
2b	1910 (vs), 1835 (w), 1794 (s)[a]/ 1894 (vs), 1774 (vs)	–	–	592 (4340)[a] [628 in CH_2Cl_2]	+215 (90, qrev.)
2c	2016 (m), 1910 (vs), 1889 (sh), 1839 (s)/ 2020 (m), 1911 (vs), 1866 (vs), 1830 (s), 1804 (vs)	–	–	539 (5820)	+660 (115, qrev.)
2d	1917 (vs), 1834 (s), 1804 (s)/ 1912 (vs), 1830 (s), 1802 (s)	2127 (s)/ 2129 (s)	–	619 (6890)	+270 (115, qrev.)
2e	1918 (vs), 1827 (s), 1800 (s) 1911 (vs), 1826 (s), 1795 (s)	–	–	616 (6160)	+355 (100, qrev.)

[a] In CH_3CN. [b] Splitting of CO absorptions in the solid state probably due to hydrogen bonding.

resonance signals of the carbonyl group *trans* to L according to their π-acceptor strength CO > CN*t*Bu > PPh_3 > CH_3CN.[14] The correlation of ^{95}Mo and ^{13}C (*trans* to L) chemical shifts is acceptably linear ($R^2=0.9584$; see Supporting Information), while no linear correlation is observed between the ^{95}Mo shift and other ^{13}CO resonance signals. Neither does there exist a linear correlation between $\delta(^{95}Mo)$ and the lowest energy absorption λ_{max} (Table 3), suggesting that the paramagnetic shielding term σ_{para} is not only influenced by the average electronic excitation energy ΔE but also by nephelauxetic contributions.[12e, 15] This is not unexpected as very different ligands concerning electronic and steric properties are considered.[16] The linewidth of the ^{95}Mo signal allows the detection of the scalar coupling to ^{31}P in complex **2e**, giving a doublet with $^1J_{Mo,P}=138$ Hz similar to that of comparable complexes.[12f, 13]

The seven-coordinate complex **1f**[17] is fluxional at room temperature preventing the observation of ^{13}C NMR signals

of the carbonyl groups at 300 K, while at 193 K three resonance signals are observed. The resonance signal of the tin atom in **1f** can be seen in the ^{119}Sn NMR spectrum at $\delta =$ 30 both at 300 and 193 K. The coordination shift amounts to 334 ppm relative to phenyltin trichloride ($\delta = -304$). No signal from the molybdenum nucleus could be observed in the ^{95}Mo NMR spectrum of **1f** at 300 K or at 193 K.

The IR spectra in solution (Table 3) are consistent with a disturbed local C_{3v} symmetry of the *fac* complexes **1b**,**1d**–**f**, **2b**, **2d**–**e** (splitting of the "E" band) and with disturbed local C_{2v} symmetry of the *cis*-tetracarbonyl complexes **1c** and **2c**. For **1f** only one set of absorption bands is observed indicting that only one isomer is formed in solution.[17]

The electronic spectra of **1b**–**1e** show metal-to-ligand charge transfer (MLCT) absorption bands in the 590–630 nm range (Table 3). According to the literature[12] these bands can be assigned to the (ligand-π*) ← (metal-d) transition. Substitution of CO by L shifts this band to lower energy, as the metal d-orbitals are more destabilised by L than by CO. For **1f** the MLCT band[17] is found at 474 nm.

The same argument holds for the interpretation of the cyclic voltammograms: the destabilisation of the metal d orbital is reflected in lower oxidation potentials for complexes with L ≠ CO (Table 3). The seven-coordinate Mo^{II} complex **1f** is irreversibly reduced at −850 mV (vs. SCE) with a new oxidation wave appearing in the reverse scan at +40 mV (vs. SCE).

Reactivity studies in solution show that ligand exchange reactions proceed in a facile way (Scheme 7). The order of increasing lability $CNtBu < CO < PPh_3 < CH_3CN$ has been established by IR and NMR spectroscopy.

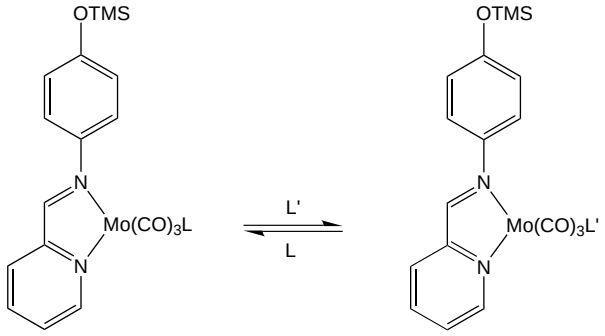

Scheme 7. Ligand-exchange reactions.

Solid-phase chemistry, resin functionalisation: Before starting to study organometallic reactions on the solid phase it is necessary to introduce a linker between the resin and the metal complex (see Scheme 1). This linker has to fulfil several requirements: 1) stability during all reactions performed on the solid phase and 2) mild cleavage conditions with reagents compatible with the final metal complex. One possible candidate is a linker based on a silyl ether[18, 19] that is stable under basic and acidic reaction conditions but can be cleaved with fluoride ions, which are expected to be unreactive towards most metal complexes.

The polystyrene resin was functionalised with a silyl chloride group (Scheme 8) according to a literature procedure.[18] Loading with the phenolic ligand **1a** is accomplished

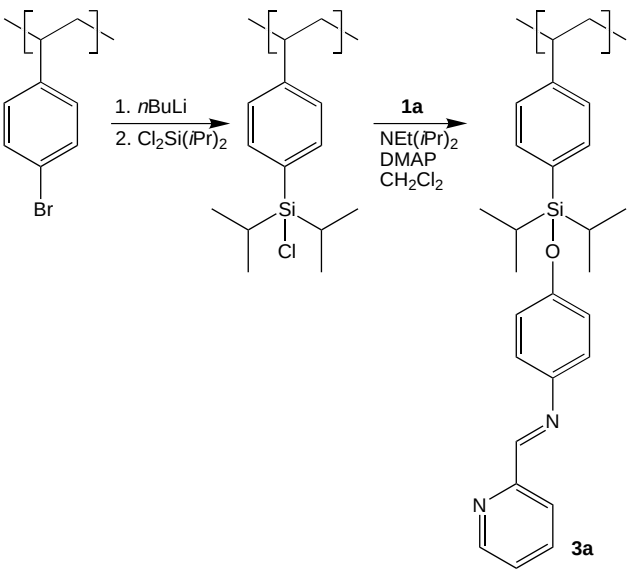

Scheme 8. Synthesis of resin **3a**.

under basic conditions (Scheme 8). The yellow ligand modified resin **3a** was studied by gel-phase ^{13}C NMR, IR, diffuse reflectance spectroscopy, and mass spectrometry to characterise the attached ligand and by differential scanning calorimetry, thermogravimetry, and studies of the swelling properties to characterise the bulk material. Quantitative loading with ligand **1a** was determined by elemental analysis (nitrogen content; 0.56 mmol **1a** per gram polymer) and metal ion uptake ($CoCl_2$ in THF; measured spectrophotometrically at 590 and 683 nm; 0.52 mmol g^{-1}). The (within error) identical results obtained by both methods indicate that all ligand sites within the polymer are accessible for metal complexation (in THF). The loading of about 0.5 mmol g^{-1} corresponds to a statistical substitution of every tenth styrene residue with the ligand **1a**.

The swelling properties of polystyrene resins have been shown to be crucial for rapid and complete transformations. The most suitable solvents (Table 4) for resin **3a** were CH_2Cl_2, THF, and toluene (2.5 mL g^{-1}) followed by *N*,*N*-dimethylacetamide (DMA) (2.2 mL g^{-1}), ethyl acetate, and CH_3CN (2.0 mL g^{-1}). In contrast to polystyrene (with 2% divinylbenzene (DVB)) the swelling of **3a** is much poorer, probably because of additional cross-linking during the reaction with $Cl_2Si(iPr)_2$ (Scheme 8). It has been proposed that swelling values greater than 4 mL g^{-1} indicate good and values of 2.0–4.0 mL g^{-1} indicate only moderate swelling properties.[20]

Although swelling of **3a** is rather poor, a gelphase ^{13}C NMR spectrum could be obtained in [D$_8$]THF, which only shows signals of the linker group and the attached ligand (Table 4) as these residues are the most mobile groups.

The covalent attachment of the linker and the ligand is also confirmed by EI mass spectrometry[18] as characteristic signals of styrene fragments containing the linker and the ligand are observed, for example $[C_8H_7Si(iPr)_2OL]^+$ at *m/z* 415 (see Experimental Section).

The IR spectrum of **3a** (as CsI disk) shows signals in addition to the signals of the polystyrene backbone due to the

0947-6539/01/0713-2926 $ 17.50+.50/0 *Chem. Eur. J.* **2001**, *7*, No. 13

Table 4. Analytical data for resins **3a–f**.

Color		**3a** yellow	**3b** blue	**3c** purple	**3d** blue	**3e** blue–green	**3f** orange-red
DRS-UV (PTFE)	λ_{max} [nm]	396	407, 775	404, 604	404, 681	412, 681	449, 533 (sh)
IR (CsI)	CH_{imine}	2726 (w)	2726 (w)	2727 (w)	2728 (w)	2722 (w)	2728 (w)
$\tilde{\nu}$/	$C{=}N_{imine}$	1627 (m)	1627 (m)	1627 (m)	1627 (m)	n. o.	1637 (m)
[cm^{-1}]	pyridine	1584 (m)	1584 (m)	1584 (m)	1586 (m)	1586 (sh)	1584 (sh)
	CO	–		2013 (s)		[a]	
		–	1911 (vs)	1909 (vs)	1921 (vs)	1911 (vs)	2008 (s)
		–	1850 (s)	1896 (sh)	1848 (s)	1847 (s)	1930 (s)
		–	1811 (s)	1851 (s)	1821 (s)	1813 (s)	1912 (s)
	CN*t*Bu	–	–	–	2112 (m)	–	–
^{13}C NMR	$Si{-}CHCH_3$	18	[d]	18	18	18	16
δ ([D_8]THF)	C^2, C^3, C^5, C^6, C^{11}	121–125		120–125	120–126	121–123	br
	C^7	158		155	159	n. o.	n. o.
	C^9	129		129	129	129	130
	C^{10}	136		137	138	138	138
	C^{12}	151		149	n. o.	n. o.	n. o.
	ligand	–		–	31 (CH_3)	126, 129, 134	126, 130, 138
^{31}P δ ($\Delta\nu_{1/2}$)		–	–	–	–	40 (1000)	–
^{119}Sn δ ($\Delta\nu_{1/2}$)		–	–	–	–	–	50 (9140)[e]
DSC	T [°C][b]		382 (sh)	385 (sh)	381 (sh)	381 (sh)	
	[$kJ\,g^{-1}$]	434 (–0.48)	421 (–0.23)	421 (–0.33)	422 (–0.35)	421 (–0.33)	425 (–0.34)
TG	T [°C][c]		117 (6)	111 (3)	104 (4)	119 (3)	113 (6)
	(weight		323 (25)	331 (25)	343 (32)	339 (27)	344 (40)
	loss/%)	358 (59)	390 (13)	399 (15)	401 (12)	402 (18)	394 (7)
			448 (19)	464 (19)	486 (15)	480 (15)	
		565 (33)	502 (30)	546 (31)	531 (30)	582 (30)	512 (40)
		8% residue	7;% residue	7% residue	7% residue	7% residue	7% residue
swelling	dry	1.6	1.6	1.6	1.5	1.5	1.5
[$mL\,g^{-1}$]	THF	2.5	2.3	2.2	2.3	2.2	2.2
	toluene	2.5	2.2	2.2	2.2	2.1	2.0

[a] In some preparations a band at 2013 cm^{-1} is observed indicating partial formation of the tetracarbonyl complex **3c**. [b] Peak maximum. [c] Inflection point. [d] Side reaction in THF prevents acquisition of NMR spectra. [e] At 203 K.

attached ligand at 2726 cm^{-1} (CH_{imine}), 1627 cm^{-1} ($C{=}N_{imine}$) and 1584 cm^{-1} (pyridine vibration). In the diffuse reflectance spectrum (measured in polytetrafluoroethylene, PTFE) a band around 400 nm is observed which is responsible for the yellow colour of the resin (Table 4, Figure 2).

The TG measurement of **3a** shows a two-step weight loss at 358 °C (59%) and 565 °C (33%); the remaining material (8%) being SiO_2.[18] Differential scanning calorimetry (DSC) of **3a** shows an endothermic process at 434 °C (–0.48 $kJ\,g^{-1}$). Both measurements indicate that attachment of the linker and the ligand to the polystyrene has an influence on the thermal properties (depolymerisation) of the bulk polymer.[18]

Solid-phase chemistry, resin complexation: Although CH_2Cl_2 was found to be a "good solvent" for swelling resin **3a**, performing the complexation of the polymer in this solvent leads to formation of the immobilised tetracarbonyl complex **3c** instead of the desired tricarbonyl complex **3b** (Scheme 4). This behaviour is analogous to the solution reaction (Scheme 5). The use of pure acetonitrile—a rather poor solvent for resin **3a**—leads to formation of the tricarbonyl complex **3b** but only with a low yield as shown by IR spectroscopy. This can be explained by the assumption that not all ligand sites are available when the resin is swollen in acetonitrile. Therefore a 1:1 mixture of toluene/acetonitrile was used (swelling 2.3 $mL\,g^{-1}$) for preparing the tricarbonyl complex **3c** on the solid phase. Immediately after the addition of the precursor complex [$(CH_3CN)_3Mo(CO)_3$] to the swollen

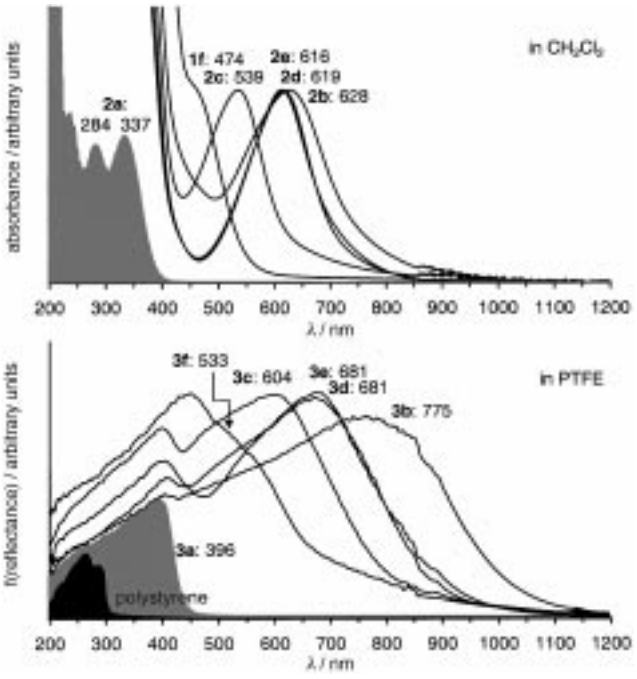

Figure 2. UV/Vis/NIR spectra of soluble (top) and immobilised complexes (bottom).

resin **3a** at room temperature the colour of the resin changes to deep blue, indicating formation of the immobilised complex while the solution remains yellow—the colour of the

starting material—demonstrating the stability of the resin-linker-ligand bonds.

As mild reaction conditions are used, formation of [(η^6-polystyrene)$Mo(CO)_3$][21] is effectively prevented as evidenced by IR spectroscopy of resin **3b** and by a blank experiment using unmodified polystyrene and $[(CH_3CN)_3Mo(CO)_3]$ at ambient temperature.

Stirring resin **3b** in CH_2Cl_2 for 7 h gives the immobilised tetracarbonyl complex **3c** (according to colour and IR spectroscopy) in close analogy to the model reactions in solution (Scheme 5)—even the rate is similar (90% yield at 6.4 h in solution). Ligand substitution reactions were therefore performed in pure toluene, which is a suitable solvent for both the resin and the ligands L (Scheme 4).

Bubbling carbon monoxide through a suspension of **3b** in toluene causes a gradual colour change of the polymer from blue to purple, giving resin **3c** while the solution remained colourless. The isonitrile ligand CN*t*Bu and the phosphane ligand PPh_3 do not cause a significant colour change of the resin. The formation of the corresponding immobilised complexes **3d** and **3e** is evidenced by spectroscopic means (see below). In all cases the toluene solution remained colourless, indicating the stability of the resin–linker and linker–ligand bonds under these conditions. From the resin-bound tetracarbonyl complex **3c** the seven-coordinate complex **3f** is formed by reaction with phenyltin trichloride (analogous to Scheme 6) again under colour change of the resin from purple to orange-red and CO evolution. In this case—unlike the solution model complex—the silyl linkage remains intact, probably because of the higher stability of the diisopropyl silylether compared with that of the trimethyl silyl group.

The easy formation of the immobilised complexes indicates that the metal moieties on the resin are accessible even for bulky ligands such as PPh_3 and $PhSnCl_3$ so that all discussed reactions on the solid phase proceed similarly to their solution counterparts.

The stability of the different resin bound complexes **3b**–**3e** towards ligand exchange follows the same trend of increasing lability as the soluble complexes CN*t*Bu < CO < PPh_3 < CH_3CN as shown by IR and ^{31}P NMR spectroscopy and cleavage from the resin (see below).

Solid-phase chemistry, resin characterisation: Unlike the pure organic resin **3a** with solely covalent bonds between main group elements, mass spectrometry of the metal complex functionalised resins **3b**–**3f** did not prove useful as the complexes decompose prior to resin depolymerisation.[18] Also elemental analysis has proven unreliable for metal containing resins as has been shown previously.[22]

For characterising the bulk material TG and DSC was used: DSC shows a shift of the peak maximum to lower temperature (9–13 °C; see Table 4) compared with that of **3a** and the TG experiments show multistep weight losses starting around 100 °C, indicating the lower thermal stability of **3b**–**3e** compared with resin **3a**. The swelling of the bulk material is slightly lower than that of the organic polymer **3a** but this might only reflect the increased mass of the polymer. Again THF and toluene are the most suitable solvents for these resins.

The most useful spectroscopic method for studying the metal complex functionalised resins **3b**–**3f** is IR spectroscopy (Table 4), especially in combination with a comparison to the spectra of the corresponding soluble complexes. In all cases the IR spectra (carbonyl region) of the immobilised complexes closely resemble those of the model complexes in solution (Figure 3). The similarity of corresponding spectra is much less when comparing the solid-state spectra indicting a "solution-like" environment for the immobilised complexes.

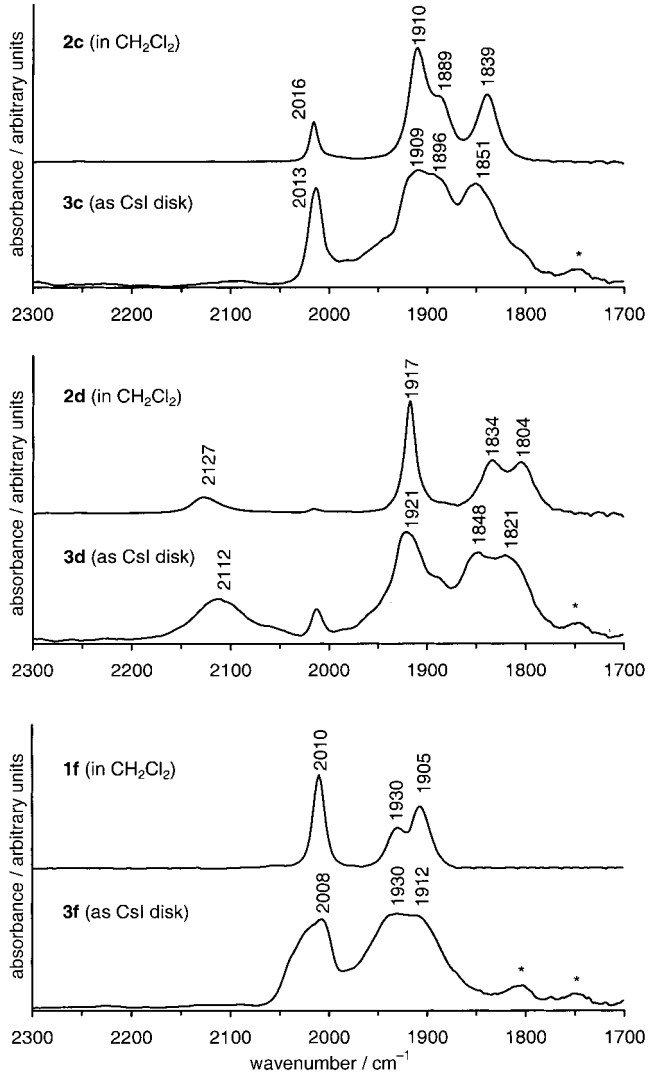

Figure 3. IR spectra of selected soluble and immobilised complex pairs (top: **2c**/**3c**; middle: **2d**/**3d**; bottom: **1f**/**3f**). Bands marked with an asterisk belong to vibrations of the polystyrene.

In addition to the strong carbonyl absorptions of the metal complexes the characteristic absorptions of the ligand-functionalised polymer are also seen around 2727, 1627, and 1584 cm^{-1} (Table 4). For resin **3d** the $\tilde{\nu}_{CN}$ of the coordinated isonitrile ligand is observed at 2112 cm^{-1}.

In the diffuse reflectance spectra of the resins **3b**–**3f** the MLCT bands are observed in the visible region (Table 4). Compared with their solution counterparts all absorption

0947-6539/01/0713-2928 $ 17.50+.50/0 *Chem. Eur. J.* **2001**, *7*, No. 13

bands are shifted to lower energy by 1500–3000 cm^{-1} but preserve the trend $\lambda_{max}(\mathbf{b}) > \lambda_{max}(\mathbf{d}) \approx \lambda_{max}(\mathbf{e}) > \lambda_{max}(\mathbf{c}) > \lambda_{max}(\mathbf{f})$ (Tables 3 and 4, Figure 2). The linear correlation between $\tilde{\nu}_{max}$ of the soluble and the immobilised complexes and ligands is very good $\tilde{\nu}_{max}$(immobilised molecules) = $\tilde{\nu}_{max}$(soluble molecules) × 0.83+924 cm^{-1} ($R^2 = 0.9801$; see Supporting Information).

The gel-phase ^{13}C NMR spectra of the polymers **3c**–**3f** show signals due to the linker and the attached ligand (Table 4). For **3d**–**3f** signals due to the monodentate ligands CN*t*Bu, PPh_3, and $PhSnCl_3$ are also seen. In the gel-phase ^{31}P NMR spectrum of **3e** the signal of coordinated phosphane ligand appears at $\delta = 40$ as a broad signal (Figure 4). The half

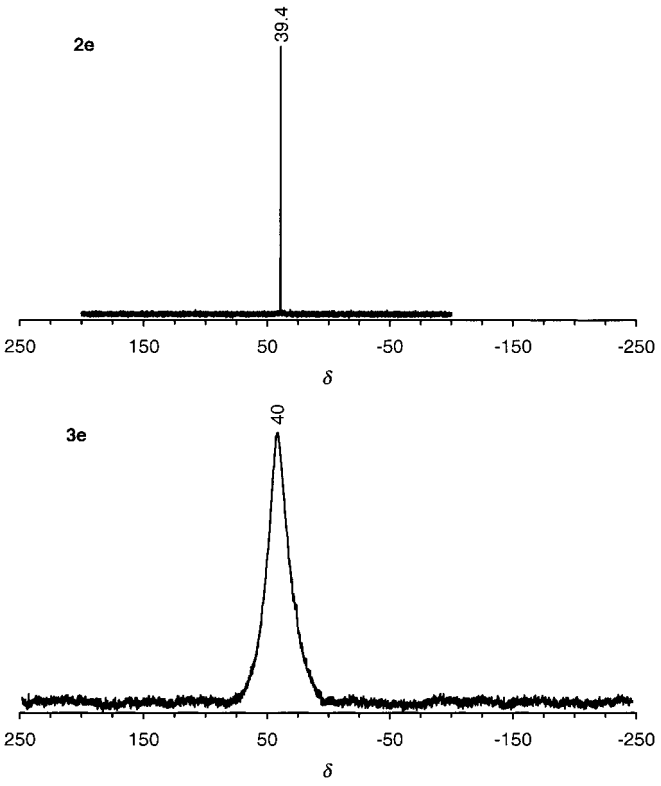

Figure 4. ^{31}P NMR spectra of **2e** (in CD_2Cl_2) and **3e** (in[D_8]THF).

width at half height is 250 times higher than in the ^{31}P NMR spectra of the soluble complexes **1e** and **2e**, indicating that this signal indeed corresponds to a polymer-bound species with much lower mobility.

An attempt to observe the ^{119}Sn signal of **3f** at room temperature failed. At −70 °C a broad signal occurs around $\delta = 50$. Its half width at half height is 35 times larger than that of the soluble analogue **1f**, again indicating the observation of a polymer-bound species.

Attempts to obtain reliable ^{95}Mo NMR spectra of the resin bound complexes failed because of the low sensitivity of the ^{95}Mo nucleus and the significant "baseline ringing" in these experiments.[15a]

In summary TG, DSC, and elemental analyses are not especially helpful in characterising the polymer-bound complexes as most of the measured quantities arise from the polymer backbone and not from the complexes of interest. In

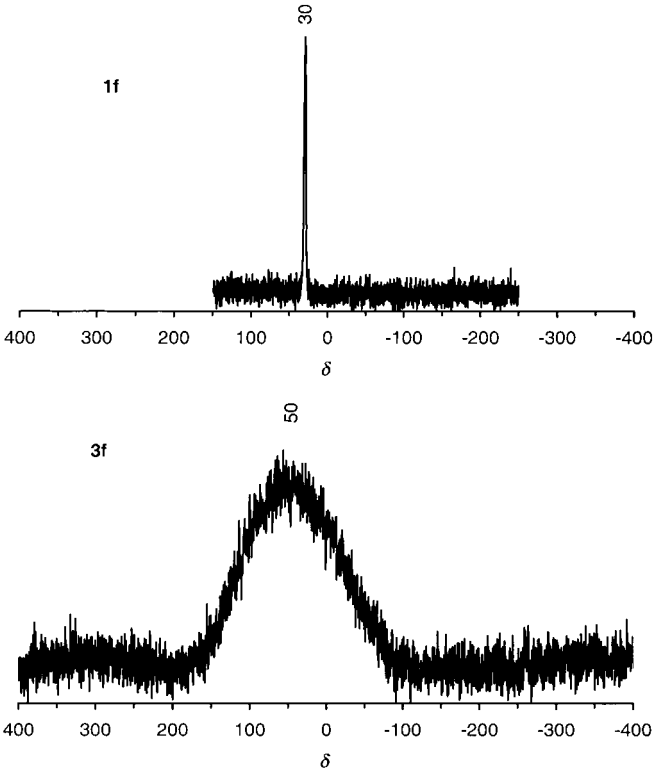

Figure 5. ^{119}Sn NMR spectra of **1f** and **3f** (in[D_8]THF).

contrast IR, diffuse reflectance, and NMR spectroscopy combine specificity for the metal complexes with the required sensitivity.

Solid-phase chemistry, cleavage: After having characterised the polymer-bound complexes directly on the solid support, we obtained indirect proof of identity through the possibility of mild cleavage of the complexes from the insoluble polymer (Scheme 9). Treating resins **3c**–**3f** with two equivalents of

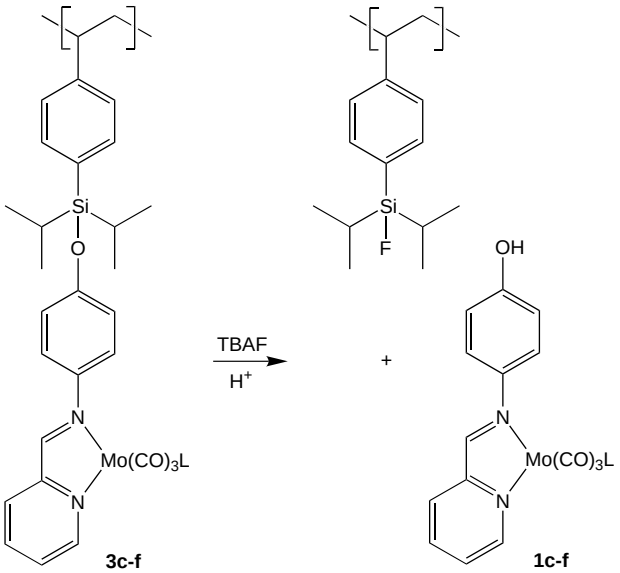

L = CO (**c**), CN*t*Bu (**d**), PPh_3 (**e**), Cl, $SnCl_2Ph$ (**f**)

Scheme 9. Cleavage of the complexes from solid support.

tetra-*n*-butylammonium fluoride in CH_2Cl_2 gives deeply coloured solutions of the deprotonated complexes. After washing the resins and concentrating the filtrates, careful acidification (at low pH the complexes start to decompose) of the solutions with acetic acid gives solutions of the respective complexes as evidenced by UV/Vis/NIR and IR spectroscopy in 30–40% yield over all steps based on the loading of **3a**. In all cases only the desired complexes are isolated with no indication of side products.

The IR spectra of the remaining slightly coloured resins prove the absence of carbonyl groups confirming quantitative cleavage from the resin. Additionally, mass spectrometry of the resins (Scheme 9) confirms the absence of attached ligands and the presence of silyl fluoride groups on the polymer.

Conclusion

Inorganic chemistry on the solid organic polystyrene phase is similar to solution chemistry of the investigated substitution and oxidative elimination reactions. Resin-bound ligands and complexes can be prepared and analysed and are readily cleaved from the solid support. Ligand substitution reactions and oxidative eliminations proceed somewhat more slowly on solid support compared to the homogeneous reaction. Care has to be taken when choosing the optimal solvent. The relative stability trend of the polymer-bound complexes is identical to that of the solution analogues. IR, DRS-UV, and NMR prove valuable to monitor the solid-phase reaction and to characterise the resin bound complexes. Finally, the investigated cleavage conditions are mild enough to obtain the free complexes from the solid support without major decomposition. With this knowledge it should now be possible to prepare inorganic and organometallic complexes on the solid phase, which might be accessible only with difficulty or even not at all in the homogeneous phase. Additionally, this methodology might be useful for combinatorial catalyst libraries when the catalysts must be tested in solution and therefore be cleaved from the support.

Experimental Section

Polystyrene (2% DVB), brominated polystyrene (2% DVB, 2.5 mmol $Br\,g^{-1}$), $Cl_2Si(iPr)_2$, *n*BuLi in toluene (2.5 M), diisopropylethylamine, (dimethylamino)pyridine (DMAP), and $nBu_4NF\cdot 3H_2O$ (TBAF) were purchased from Fluka, phenyltin trichloride from Strem. The polystyrene resins were washed prior to use with CCl_4, acetone, acetone/H_2O (2:1), acetone, benzene, MeOH, CH_2Cl_2, and diethyl ether and dried under vacuum. Unless noted otherwise, all manipulations were carried out under argon by means of standard Schlenk techniques. All solvents were dried by standard methods and distilled under argon prior to use. All other reagents were used as received from commercial sources. For the solid-phase reactions a flask with a nitrogen inlet and a coarse porosity fritted glass filter that allows addition and removal of reagents and solvents without exposure of the resin to the atmosphere was used.

NMR spectra were obtained on a Bruker Avance DPX 200 (200.15 MHz (^{1}H), 50.323 MHz (^{13}C), 81.015 MHz (^{31}P), 13.029 MHz (^{95}Mo), 74.630 MHz (^{119}Sn)) at 303 K if not noted otherwise; chemical shifts (δ) are reported in ppm with respect to residual solvent peaks as internal standards: [D_8]THF (^{1}H: $\delta = 1.73$; ^{13}C: $\delta = 25.5$), CD_3CN (^{1}H: $\delta = 1.93$; ^{13}C: $\delta = 1.3$), CD_2Cl_2 (^{1}H: $\delta = 5.32$; ^{13}C: $\delta = 53.8$); [d_6]DMSO (^{1}H: $\delta = 2.50$; ^{13}C: $\delta = 39.4$). ^{31}P chemical shifts (δ) in ppm with respect to 85% H_3PO_4 (^{31}P: $\delta = 0$), ^{95}Mo chemical shifts (δ) in ppm with respect to 1 M Na_2MoO_4 in D_2O (^{95}Mo: $\delta = 0$) and ^{119}Sn chemical shifts (δ) in ppm with respect to $SnMe_4$ in THF (^{119}Sn: $\delta = 0$) as external standards. IR spectra were recorded on a BioRad Excalibur FTS 3000 spectrometer using caesium iodide disks or CaF_2 cells. UV/Vis/NIR spectra were recorded on a Perkin Elmer Lambda 19 in 0.2 cm cells (Hellma, suprasil). DRS spectra were measured with the same instrument using the Perkin Elmer integrating sphere and polytetrafluoroethylene (PTFE) as reference. Mass spectra were recorded on a Finnigan MAT 8400 spectrometer, electron energy 70 eV (EI), 4-nitrobenzyl alcohol matrix (FAB). Elemental analyses were performed by the microanalytical laboratory of the Organic Chemistry Department, University of Heidelberg. Cyclic voltammetry was performed on a Metrohm "Universal Meß- und Titriergefäß", Metrohm GC electrode RDE 628, platinum electrode, SCE electrode, Princeton Applied Research potentiostat Model 273; substrate concentration 10^{-3} M in 0.1 M nBu_4NPF_6/CH_2Cl_2 or in 0.1 M nBu_4NPF_6/CH_3CN. All potentials are given relative to that of SCE. Differential scanning calorimetry measurements were carried out on a Mettler DSC 30, heating rate 10 K min^{-1}, under argon from 30–600 °C. Thermogravimetric measurements were carried out on a Mettler TC 15, heating rate 10 K min^{-1} under argon from 30–800 °C. Swelling measurements were performed by weighing a known amount of resin into a calibrated NMR tube and adding excess solvent. The volume of the swollen resin was measured after 3 h.

4-[(Pyridine-2-ylmethylene)amino]phenol (1a): Pyridine-2-carbaldehyde (15 g, 140.2 mmol), *p*-aminophenol (15.3 g, 140.2 mmol), $MgSO_4$ (8 g) and ethyl acetate (120 mL) were heated under reflux for 2 h. The solvent was removed under reduced pressure and the yellow residue was taken up in water and extracted with *n*-butanol (3 ×). The alcohol was removed under reduced pressure and the yellow solid residue washed with water (3 ×) and diethyl ether (3 ×) and dried in vacuo, yielding **1a** (25 g, 126 mmol; 90%). ^{1}H NMR (200 MHz, [D_6]DMSO): $\delta = 6.86$ (d, $^3J_{H,H} = 8.7$ Hz, 2H; $H^{3,5}$), 7.32 (d, $^3J_{H,H} = 8.7$ Hz, 2H; $H^{2,6}$), 7.49 (pt, 1H; H^{11}), 7.93 (pt, 1H; H^{10}), 8.14 (d, $J_{H,H} = 7.8$ Hz, 1H; H^9), 8.62 (s, 1H; H^7), 8.70 (d, $J_{H,H} = 4.6$ Hz, 1H; H^{12}), 9.63 (s, 1H; OH); ^{13}C NMR (50 MHz, [D_6]DMSO): $\delta = 116.7$ (s; $C^{3,5}$), 121.6 (s; C^9), 123.8 (s; $C^{2,6}$), 125.9 (s; C^{11}), 137.7 (s; C^{10}), 142.4 (s; C^1), 150.4 (s; C^{12}), 155.5 (s; C^4), 157.8 (s; C^7), 158.0 (s; C^8) All signals were assigned on the basis of DEPT, CH-COSY and NOESY experiments. The conformations in solution are *transoid* as no cross peaks between H^7 and H^9 (numbering scheme shown in Scheme 2) are observed in the NOESY spectra; IR (CsI): $\tilde{\nu} = 3040-2472$ (m, br, OH, CH), 1626 (m), 1601 (m), 1581 (s), 1510 (s) cm^{-1}; UV/Vis (CH_2Cl_2): λ_{max} (ε) = 286 (15560), 340 nm (19740 $M^{-1}cm^{-1}$); MS (EI, 70 eV): *m/z* (%): 198 (100) $[M]^+$, 181 (2) $[M^+ - OH]^+$, 171 (45) $[M - HCN]^+$, 154 (3) $[M - OH - HCN]^+$, 79 (26) $[C_5H_5N]^+$; elemental analysis (%) calcd for $C_{12}H_{10}N_2O$ (198.22): C 72.71, H 5.08, N 14.13; found: C 72.62, H 5.09, N 14.08.

Pyridine-2-ylmethylene-(4-trimethylsilanyloxyphenyl)amine (2a): A suspension of **1a** (2.97 g, 15 mmol) in THF (30 mL) was cooled to 0 °C. NEt_3 (1.57 g, 15.5 mmol) was added through a cannula. After the mixture had been stirred for 10 min, TMSCl (1.68 g, 15.5 mmol) was added and the suspension was stirred for 1 h at 0 °C and 1 h at 25 °C. The solvent was removed under reduced pressure and the yellow residue dissolved in diethyl ether. The yellow solution was filtered and the solvent removed under reduced pressure to give **2a** as an orange-yellow oil (3.53 g, 87%). ^{1}H NMR (200 MHz, CD_2Cl_2): $\delta = 0.38$ (s, 9H; CH_3), 6.99 (d, $^3J_{H,H} = 8.8$ Hz, 2H; $H^{3,5}$), 7.36 (d, $^3J_{H,H} = 8.8$ Hz, 2H; $H^{2,6}$), 7.40 (pt, 1H; H^{11}), 7.84 (pt, 1H; H^{10}), 8.28 (d, $J_{H,H} = 8.0$ Hz, 1H; H^9), 8.71 (s, 1H; H^7), 8.74 (d, $J_{H,H} = 4.6$ Hz, 1H; H^{12}); ^{13}C NMR (50 MHz, CD_2Cl_2): $\delta = 0.37$ (s; CH_3), 121.1 (s; $C^{3,5}$), 121.6 (s; C^9), 123.0 (s; $C^{2,6}$), 125.2 (s; C^{11}), 136.9 (s; C^{10}), 144.9 (s; C^1), 149.9 (s; C^{12}), 155.1 (s; C^4), 155.5 (s; C^8), 159.1 (s; C^7); IR (CsI): $\tilde{\nu} = 3060$ (w, CH_{Ar}), 2960 (m, CH_3), 1627 (m), 1597 (w), 1583 (s), 1503 (vs) cm^{-1}; UV/Vis (CH_2Cl_2): λ_{max} (ε) = 285 (21810), 337 nm (23230 $M^{-1}cm^{-1}$); MS (EI, 70 eV): *m/z* (%): 270 (100) $[M]^+$, 269 (70) $[M - H]^+$, 255 (12) $[M - CH_3]^+$; elemental analysis (%) calcd for $C_{15}H_{18}N_2OSi$ (270.41): C 66.62, H 6.71, N 10.36; found: C 66.52, H 6.67, N 10.59.

***fac*-Tricarbonyl(2a)(acetonitrile)molybdenum(0) (2b)**: [$(CH_3CN)_3Mo(CO)_3$] (303 mg, 1 mmol) was treated with **2a** (270 mg, 1 mmol) in CH_3CN (20 mL) to give an intensely turquoise-coloured solution. After stirring for 3 h at room temperature the solution was concentrated to about 5 mL and petroleum ether (PE) 40/60 (40–50 mL) was added. After 24 h the

  0947-6539/01/0713-2930 $ 17.50+.50/0 *Chem. Eur. J.* **2001**, *7*, No. 13

coloured solution was removed with a cannula and the dark residue was washed with PE 40/60 and dried in vacuo to give **2b** as a purple powder (417 mg; 85%). The reaction can also be performed on a 10 mmol scale. MS (FAB): *m/z* (%): 452 (78) $[M-CH_3CN]^+$, 424 (20) $[M-CH_3CN-CO]^+$, 396 (60) $[M-CH_3CN-2\,CO]^+$, 368 (100) $[M-CH_3CN-3\,CO]^+$; elemental analysis (%) calcd for $C_{20}H_{21}N_3O_4SiMo$ (491.43): C 48.68, H 4.29, N 8.52; found: C 48.30, H 4.33, N 8.50.

***cis*-Tetracarbonyl(2a)molybdenum(0) (2c)**: Carbon monoxide was bubbled into a solution of **2b** (491 mg, 1 mmol) in CH_2Cl_2 (20 mL) until the IR spectrum showed only the presence of **2c** resulting in a purple solution. The reaction mixture was stirred under a CO atmosphere for 1 h. Removal of the solvent in vacuo left **2c** as a purple powder (477 mg; 100%). MS (FAB): *m/z* (%): 480 (45) $[M]^+$, 452 (100) $[M-CO]^+$, 424 (20) $[M-2\,CO]^+$, 396 (30) $[M-3\,CO]^+$, 368 (40) $[M-4\,CO]^+$; elemental analysis (%) calcd for $C_{19}H_{18}N_2O_5SiMo$ (478.39): C 47.70, H 3.79, N 5.86; found: C 47.30, H 3.87, N 6.07.

***fac*-Tricarbonyl(2a)(*tert*-butyl isonitrile)molybdenum(0) (2d)**: *tert*-Butyl isonitrile (0.11 mL, 1 mmol) was added to a solution of **2b** (491 mg, 1 mmol) in CH_2Cl_2 (20 mL) to give a deep blue solution. After stirring for 3 h at room temperature the solution was concentrated to about 5 mL and PE 40/60 (40–50 mL) was added. After 24 h the coloured solution was removed with a cannula and the dark blue residue was washed with PE 40/60 and dried in vacuo to give **2d** as a blue powder (470 mg; 88%). MS (FAB): *m/z* (%): 535 (10) $[M]^+$, 507 (50) $[M-CO]^+$, 479 (18) $[M-2\,CO]^+$, 451 (30) $[M-3\,CO]^+$, 368 (100) $[M-3\,CO-CNtBu]^+$; elemental analysis (%) calcd for $C_{23}H_{27}N_3O_4SiMo$ (533.51): C 51.78, H 5.10, N 7.88; found: C 50.55, H 4.86, N 7.78.

***fac*-Tricarbonyl(2a)(triphenylphosphane)molybdenum(0) (2e)**: Triphenylphosphane (262 mg, 1 mmol) was added to a solution of **2b** (491 mg, 1 mmol) in CH_2Cl_2 (20 mL), giving a deep blue solution. After stirring for 3 h at room temperature the solution was concentrated to about 5 mL and PE 40/60 (40–50 mL) was added. After 24 h the coloured solution was removed with a cannula and the dark blue residue was washed with PE 40/60 and dried in vacuo to give **2e** as a blue powder (640 mg, 90%). MS (FAB): *m/z* (%): 714 (33) $[M]^+$, 686 (80) $[M-CO]^+$, 658 (30) $[M-2\,CO]^+$, 630 (100) $[M-3\,CO]^+$; elemental analysis (%) calcd for $C_{36}H_{33}N_2O_4SiPMo$ (712.67): C 60.67, H 4.66, N 3.93, P 4.35; found: C 60.40, H 4.75, N 4.01, P 4.30.

***fac*-Tricarbonyl(1a)(acetonitrile)molybdenum(0) (1b)**: The preparation was similar to that of **2b** but **1a** (198 mg, 1 mmol) was used. The washing solution was almost colourless. Yield: 385 mg (92%). MS (FAB): *m/z* (%): 380 (100) $[M-CH_3CN]^+$, 352 (24) $[M-CH_3CN-CO]^+$, 324 (46) $[M-CH_3CN-2\,CO]^+$; elemental analysis (%) calcd for $C_{17}H_{13}N_3O_4Mo$ (419.25): calcd: C 48.70, H 3.13, N 10.02; found: C 48.08, H 3.15, N 9.87.

***cis*-Tetracarbonyl(1a)molybdenum(0) (1c)**: The preparation was similar to that of **2c** but **1b** (419 mg, 1 mmol) was used instead of **2b**. Yield: 405 mg (100%). MS (FAB): *m/z* (%): 408 (47) $[M]^+$, 380 (100) $[M-CO]^+$; elemental analysis (%) calcd for $C_{16}H_{10}N_2O_5Mo$ (406.21): C 47.31, H 2.48, N 6.90; found C 46.90, H 2.80, N 6.85.

***fac*-Tricarbonyl(1a)(*tert*-butyl isonitrile)molybdenum(0) (1d)**: The preparation was similar to that of **2d** but **1b** (419 mg, 1 mmol) was used instead of **2b**. Yield: 435 mg (94%). MS (FAB): *m/z* (%): 463 (65) $[M]^+$, 435 (100) $[M-CO]^+$; elemental analysis (%) calcd for $C_{20}H_{19}N_3O_4Mo$ (461.33): C 52.07, H 4.15, N 9.11; found: C 51.37, H 4.12, N 9.00.

***fac*-Tricarbonyl(1a)(triphenylphosphane)molybdenum(0) (1e)**: The preparation was similar to that of **2e** but **1b** (419 mg, 1 mmol) was used instead of **2b**. Yield: 430 mg (93%). Recrystallisation from CH_2Cl_2/Et_2O afforded dark blue crystals. MS (FAB): *m/z* (%): 642 (48) $[M]^+$, 614 (80) $[M-CO]^+$, 586 (100) $[M-2\,CO]^+$, 557 (91) $[M-3\,CO-H]^+$; elemental analysis (%) calcd for $C_{33}H_{25}N_2O_4PMo$ (640.49) · 0.5 Et_2O: C 62.05, H 4.46, N 4.13, P 4.57; found: C 61.73, H 4.53, N 4.23, P 4.52.

μ-Chloro-(dichlorophenyltin)–(1a)tricarbonyl molybdenum(0) (1f): Phenyltin trichloride (606 mg, 2 mmol) was added with syringe to a solution of **1c** (406 mg, 1 mmol) in acetone (20 mL). The solution was stirred for 5 h at room temperature until IR spectroscopy indicated completeness of the reaction. The colour turned from deep purple to orange-red. The solvent was removed under reduced pressure and the residue was washed with diethyl ether (6 × 20 mL) and dried to give a yellow-orange powder (550 mg; 81%). Recrystallisation from THF/Et_2O afforded orange-coloured crystals. MS (FAB): *m/z* (%): 645 (51) $[M-Cl]^+$, 561 (24) $[M-Cl-3\,CO]^+$, 380 (100) $[M-SnCl_2Ph]^+$; elemental analysis (%) calcd for $C_{21}H_{15}N_2O_4SnCl_3Mo$ (680.35) · 1.0 Et_2O: C 39.80, H 3.34, N 3.71; found: C 39.48, H 3.43, N 3.77.

Reaction of $[(CH_3CN)_3Mo(CO)_3]$ with polystyrene: $[(CH_3CN)_3Mo(CO)_3]$ (455 mg, 1.5 mmol) dissolved in CH_3CN was added to polystyrene (1 g; 2% DVB) swollen in CH_3CN/toluene (1:2). The suspension was slowly stirred at room temperature for 3 h. The solvent was removed by filtration and the resin was washed repeatedly with CH_3CN, toluene, and Et_2O until the washings were colourless. The IR spectrum (absence of ν_{CO} bands) indicated no formation of $[(polystyrene)Mo(CO)_3]$.[21]

Resin 3a: The resin was prepared from brominated polystyrene (2% DVB, 2.5 mmol Br g^{-1}) according to a published procedure[18] using the ligand **1a** to give a yellow-coloured polymer. MS (EI, 70 eV, 407 °C): *m/z* (%): 104 (100) $[C_8H_8]^+$, 329 (11) $[C_8H_7SiOL+H]^+$, 343 (43) $[C_8H_7SiMeOL]^+$, 372 (84) $[C_8H_7Si(iPr)OL]^+$, 415 (69) $[C_8H_7Si(iPr)_2OL]^+$; elemental analysis (%) calcd for $(C_8H_8)_{20}(C_{26}H_{30}SiON_2)_3(C_{15}H_{24}SiO)_7$: C 81.32, H 8.23, N 1.66; found C 78.93, H 7.38, N 1.56; which corresponds to 0.56 mmol **1a** per gram polymer. Uptake of $CoCl_2$ corresponds to 0.52 mmol per gram polymer.

Uptake of $CoCl_2$: A standard solution of $CoCl_2$ in THF was treated with a weighed amount of resin **3a**. From the decrease of the absorbances at 590 and 683 nm of the solution the loading was calculated by extrapolation to $t\rightarrow\infty$.

Resin 3b: $[(CH_3CN)_3Mo(CO)_3]$ (303 mg, 1.0 mmol) dissolved in CH_3CN (5 mL) was added to resin **3a** (1 g; corresponding to 0.56 mmol **1a**) swollen in toluene (5 mL). The suspension was allowed to stand at room temperature for 24 h with occasional stirring. The solvents were removed by filtration and the polymer was washed with CH_3CN (4 × 10 mL), toluene/CH_3CN (10 mL), toluene (2 × 10 mL), and finally with diethyl ether (2 × 10 mL). The blue resin was dried in vacuo to give a blue powder or was directly allowed to react with the ligands L (see below). Elemental analysis (%) calcd for $(C_8H_8)_{20}(C_{31}H_{33}SiO_4N_3Mo)_3(C_{15}H_{24}SiO)_7$: C 75.05, H 7.51, N 2.20; found: C 77.41, H 7.32, N 1.68.

Resin 3c: CO was bubbled for 15 min into a suspension of resin **3b** (starting from 1 g of **3a**, 0.56 mmol) swollen in toluene (6 mL). The blue resin turned purple. The suspension was allowed to stand at room temperature under CO for 24 h with occasional stirring. The solvents were removed by filtration and the polymer was washed with toluene (1 × 10 mL) and diethyl ether (2 × 10 mL). The resin was dried in vacuo giving a purple powder. Elemental analysis (%) calcd for $(C_8H_8)_{20}(C_{30}H_{33}SiO_5N_2Mo)_3(C_{15}H_{24}SiO)_7$: C 74.94, H 7.40, N 1.48; found: C 77.53, H 7.06, N 1.42.

Resin 3d: To resin **3b** (starting from 1 g of **3a**, 0.56 mmol) swollen in toluene (6 mL) CN*t*Bu (0.11 mL, 1.0 mmol) was added with a syringe. The suspension was allowed to stand at room temperature for 8 h with occasional stirring. The solvents were removed by filtration and the polymer was washed with toluene (5 × 10 mL) and diethyl ether (2 × 10 mL). The dark blue-green resin was dried in vacuo giving a dark blue-green powder. Elemental analysis (%) calcd for $(C_8H_8)_{20}(C_{34}H_{39}SiO_4N_3Mo)_3(C_{15}H_{24}SiO)_7$: C 75.28, H 7.66, N 2.15; found: C 78.61, H 7.45, N 1.66.

Resin 3e: PPh_3 (262 mg, 1.0 mmol) dissolved in toluene (3 mL) was added with a syringe to resin **3b** (starting from 1 g of **3a**, 0.56 mmol) swollen in toluene (3 mL). The suspension was allowed to stand at room temperature for 24 h with occasional stirring. The solvents were removed by filtration and the polymer was washed with toluene (5 × 10 mL) and diethyl ether (2 × 10 mL). The dark blue resin was dried in vacuo to give a dark blue powder. Elemental analysis (%) calcd for $(C_8H_8)_{20}(C_{47}H_{45}SiO_4N_2PMo)_3(C_{15}H_{24}SiO)_7$: C 76.28, H 7.30, N 1.31, P 1.46; found: C 76.71, H 6.85, N 1.29, P 0.87.

Resin 3f: Phenyltin trichloride (303 mg, 1 mmol) was added with a syringe to resin **3c** (starting from 1 g of **3a**, 0.56 mmol) swollen in toluene (6 mL). The suspension was allowed to stand at room temperature for 24 h with occasional stirring. The solvents were removed by filtration and the polymer was washed with toluene (4 × 10 mL) and diethyl ether (2 × 10 mL). The resin was dried in vacuo giving an orange-red powder. Elemental analysis (%) calcd for $(C_8H_8)_{20}(C_{35}H_{35}SiO_4N_2MoSnCl_3)_3(C_{15}H_{24}SiO)_7$: C 68.25, H 6.70, N 1.29; found: C 69.13, H 6.59, N 1.33.

Cleavage of the resin-bound complexes: Tetra-*n*-butylammonium fluoride (TBAF · 3H_2O, 315 mg, 1 mmol) in CH_2Cl_2 (5 mL) was added to the appropriate resin (starting from 1 g of **3a**, 0.56 mmol) swollen in CH_2Cl_2 (3 mL). The suspension was stirred slowly for 12 h. The coloured solution was removed by filtration and the resin was washed thoroughly with

CH_2Cl_2/Et_2O mixtures until the solutions remained colourless. The combined filtrates were dried in vacuo. Dissolving the dark residue in CH_2Cl_2 (100 mL) and careful acidification with degassed acetic acid (0.1 mL) gave intensely coloured solutions of the respective complexes. The yields were determined by UV/Vis spectrophotometry and the identities were confirmed by IR spectroscopy. Overall yields (metallation, substitution, cleavage, and acidification) based on the loading of **3a** were between 30 and 40%. After cleavage, samples of the remaining resins were subjected to mass spectrometry, which showed complete removal of the complexes. MS (EI, 70 eV, 400°C): *m*/*z* (%): 104 (100) $[C_8H_8]^+$, 151 (18) $[C_8H_7SiF+H]^+$, 165 (80) $[C_8H_7SiMeF]^+$, 193 (60) $[C_8H_7Si(i\mathrm{Pr})F]^+$, 236 (22) $[C_8H_7Si(i\mathrm{Pr})_2F]^+$.

Acknowledgements

This work was supported by the Deutsche Forschungsgemeinschaft and the Fonds der Chemischen Industrie. The permanent, generous support from Prof. Dr. G. Huttner is gratefully acknowledged.

[1] F. Zaragoza Dörwald, *Organic Synthesis on Solid Phase*, Wiley-VCH, Weinheim, **2000**.
[2] a) K. S. Schmidt, D. M. Filippov, N. J. Meeuwenoord, G. A. van der Marel, J. H. van Boom, B. Lippert, J. Reedijk, *Angew. Chem.* **2000**, *112*, 383 – 385; *Angew. Chem. Int. Ed.* **2000**, *39*, 375 – 377; b) S. I. Khan, A. E. Beilstein, M. W. Grinstaff, *Inorg. Chem.* **1999**, *38*, 418 – 419; c) S. I. Khan, A. E. Beilstein, M. Sykora, G. D. Smith, X. Hu, M. W. Grinstaff, *Inorg. Chem.* **1999**, *38*, 3922 – 3925; d) A. E. Beilstein, M. W. Grinstaff, *Chem. Commun.* **2000**, 50 – 510.
[3] M. S. Robillard, A. R. P. M. Valentijn, N. J. Meeuwenoord, G. A. van der Marel, J. H. van Boom, J. Reedijk, *Angew. Chem.* **2000**, *112*, 3226 – 3229; *Angew. Chem. Int. Ed.* **2000**, *39*, 3096 – 3099.
[4] S. Tadesse, A. Bhandari, M. A. Gallop, *J. Comb. Chem.* **1999**, *1*, 184 – 187.
[5] a) N. E. Schore, S. D. Najdi, *J. Am. Chem. Soc.* **1990**, *112*, 441 – 442; b) A. C. Comely, S. E. Gibson, N. J. Hales, *Chem. Commun.* **2000**, 305 – 306; c) A. C. Comely, S. E. Gibson, N. J. Hales, *Chem. Commun.* **1999**, 2075 – 2076; d) S. E. Gibson, N. J. Hales, M. A. Peplow, *Tetrahedron Lett.* **1999**, *40*, 1417 – 1418; e) M. F. Semmelhack, G. Hilt, J. H. Colley, *Tetrahedron Lett.* **1998**, *39*, 7683 – 7686; f) N. Mensi, S. S. Isied, *J. Am. Chem. Soc.* **1987**, *109*, 7882 – 7884; g) B. A. Arbo, S. S. Isied, *Int. J. Peptide Protein Res.* **1993**, *42*, 138 – 154.
[6] a) J. B. Arterburn, K. V. Rao, M. C. Perry, *Angew. Chem.* **2000**, *112*, 787 – 788; *Angew. Chem. Int. Ed.* **2000**, *39*, 771 – 772; b) F. Minutolo, J. A. Katzenellenbogen, *Angew. Chem.* **1999**, *111*, 1730 – 1732; *Angew. Chem. Int. Ed.* **1999**, *38*, 1617 – 1620.
[7] a) B. Altava, M. I. Burguete, J. M. Fraile, J. I. García, S. V. Luis, J. A. Mayoral, M. J. Vicent, *Angew. Chem.* **2000**, *112*, 1563 – 1566; *Angew. Chem. Int. Ed.* **2000**, *39*, 1503 – 1506; b) R. Drake, R. Dunn, D. C. Sherrington, S. J. Thomson, *Chem. Commun.* **2000**, 1931 – 1932; c) S. Tamagaki, R. J. Card, D. C. Neckers, *J. Am. Chem. Soc.* **1978**, *100*, 6635 – 6639.
[8] a) H. Miessner, K. Richter, *J. Mol. Catal. A* **1999**, *146*, 107 – 115; b) H. Miessner, *J. Am. Chem. Soc.* **1994**, *116*, 11522 – 11530; c) B. B. Kaul, R. K. Hayes, T. A. George, *J. Am. Chem. Soc.* **1990**, *112*, 2002 – 2003; d) G. Gubitosa, H. H. Brintzinger, *J. Organomet. Chem.* **1977**, *140*, 187 – 193; e) G. Gubitosa, M. Boldt, H. H. Brintzinger, *J. Am. Chem. Soc.* **1977**, *99*, 5174 – 5175; f) R. H. Grubbs, C. P. Lau, R. Cukier, C. H. Brubaker, *J. Am. Chem. Soc.* **1977**, *99*, 4517 – 4518; g) W. D. Bonds, C. H. Brubaker, E. S. Chandrasekaran, C. Gibbons, R. H. Grubbs, L. C. Kroll, *J. Am. Chem. Soc.* **1975**, *97*, 2128 – 2132; h) R. H. Grubbs, C. Gibbons, L. C. Kroll, W. D. Bonds, C. H. Brubaker, *J. Am. Chem. Soc.* **1973**, *95*, 2373 – 2375; i) S. Dahmen, S. Bräse, *Angew. Chem.* **2000**, *112*, 3827 – 3830; *Angew. Chem. Int. Ed.* **2000**, *39*, 3681 – 3683.
[9] S. Bräse, D. Enders, J. Köbberling, F. Avemaria, *Angew. Chem.* **1998**, *110*, 3614 – 3616; *Angew. Chem. Int. Ed.* **1998**, *37*, 3413 – 3415.
[10] a) B. M. Trost, I. Hachiya, *J. Am. Chem. Soc.* **1998**, *120*, 1104 – 1105; b) B. M. Trost, S. Hildbrand, K. Dogra, *J. Am. Chem. Soc.* **1999**, *121*, 10416 – 10417; c) B. M. Trost, M. Lautens, *J. Am. Chem. Soc.* **1983**, *105*, 3343 – 3344; d) B. M. Trost, M. Lautens, *J. Am. Chem. Soc.* **1982**, *104*, 5543 – 5545; e) F. Glorius, A. Pfaltz, *Org. Lett.* **1999**, *1*, 141 – 144; f) N.-F. K. Kaiser, U. Bremberg, M. Larhed, C. Moberg, A. Hallberg, *Angew. Chem.* **2000**, *112*, 3742 – 3744; *Angew. Chem. Int. Ed.* **2000**, *39*, 3596 – 3598; g) M. P. T. Sjögren, H. Frisell, B. Åkermark, P.-O. Norrby, L. Eriksson, A. Vitagliano, *Organometallics*, **1997**, *16*, 942 – 950.
[11] W. Kaim, S. Kohlmann, *Inorg. Chem.* **1987**, *26*, 68 – 77.
[12] a) H. Behrens, E. Lindner, G. Lehnert, *J. Organomet. Chem.* **1970**, *22*, 439 – 448; b) A. Srivastavsa, A. K. Shrimal, S. C. Srivastavsa, *Polyhedron* **1994**, *13*, 975 – 982; c) B. Bildstein, M. Malaun, H. Kopacka, M. Fontani, P. Zanello, *Inorg. Chim. Acta* **2000**, *300 – 302*, 16 – 22; d) L. W. Houk, G. R. Dobson, *Inorg. Chem.* **1966**, *5*, 2119 – 2123; e) M. N. Ackermann, W. G. Fairbrother, N. S. Amin, C. J. Deodene, C. M. Lamborg, P. T. Martin, *J. Organomet. Chem.* **1996**, *523*, 145 – 151; f) E. C. Alyea, V. K. Jain, *Polyhedron* **1995**, *15*, 1723 – 1730.
[13] R. W. Balk, D. J. Stufkens, A. Oskam, *Inorg. Chim. Acta* **1978**, *28*, 133 – 143.
[14] R. A. Grieves, J. Mason, *Polyhedron* **1986**, *5*, 415 – 421.
[15] a) J. Malito, *Ann. Rep. NMR Spectrosc.* **1997**, *33*, 151 – 206; b) M. Minelli, W. J. Maley, *Inorg. Chem.* **1989**, *28*, 2954 – 2958.
[16] S. Song, E. C. Alyea, *Can. J. Chem.* **1996**, *74*, 2304 – 2320.
[17] a) A. Bell, R. A. Walton, *J. Organomet. Chem.* **1985**, *290*, 341 – 352; b) R. Kummer, W. A. G. Graham, *Inorg. Chem.* **1968**, *7*, 310 – 315; c) M. Elder, W. A. G. Graham, D. Hall, R. Kummer, *J. Am. Chem. Soc.* **1968**, *90*, 2189 – 2190; d) M. Panizo, M. Cano, *J. Organomet. Chem.* **1985**, *287*, 221 – 229.
[18] K. Heinze, U. Winterhalter, T. Jannack, *Chem. Eur. J.* **2000**, 6, 4203 – 4210.
[19] a) J. T. Randolph, K. F. McClure, S. J. Danishefsky, *J. Am. Chem. Soc.* **1995**, *117*, 5712 – 5719; b) S. J. Danishefsky, K. F. McClure, J. T. Randolph, R. B. Ruggeri, *Science* **1993**, *206*, 1307 – 1309; c) L. A. Thompson, F. L. Moore, Y.-C. Moon, J. A. Ellman, *J. Org. Chem.* **1998**, *63*, 2066 – 2067.
[20] R. Santini, M. C. Griffith, M. Qi, *Tetrahedron Lett.* **1998**, *39*, 8951 – 8954.
[21] C. P. Tsonis, M. F. Farona, *J. Organomet. Chem.* **1976**, *114*, 293 – 298.
[22] R. J. Card, D. C. Neckers, *Inorg. Chem.* **1978**, *17*, 2345 – 2349.

Received: December 20, 2000 [F2955]

  0947-6539/01/0713-2932 $ 17.50+.50/0